Liquid Crystals
Publication details, including instructions for authors and subscription information:
http://www.informaworld.com/smpp/title~content=t713926090

Advantageous voltage-holding ratio characteristics induced by in-plane electric fields, and the optimization concept of liquid crystals for an in-plane switching electro-optical effect

Masahito Oh-E

Online publication date: 06 August 2010

To cite this Article Oh-E, Masahito(1998) 'Advantageous voltage-holding ratio characteristics induced by in-plane electric fields, and the optimization concept of liquid crystals for an in-plane switching electro-optical effect', Liquid Crystals, 25: 6, 699 — 709
To link to this Article: DOI: 10.1080/026782998205714
URL: http://dx.doi.org/10.1080/026782998205714

LIQUID CRYSTALS, 1998, VOL. 25, NO. 6, 699–709

Advantageous voltage-holding ratio characteristics induced by in-plane electric fields, and the optimization concept of liquid crystals for an in-plane switching electro-optical effect

MASAHITO OH-E* and KATSUMI KONDO
Hitachi Research Laboratory, Hitachi, Ltd., 7-1-1 Ohmika-cho, Hitachi-shi, Ibaraki-ken 319-12, Japan

(*Received 9 March 1998; accepted 9 June 1998*)

In-plane switching (IPS) of liquid crystals showed advantageous voltage-holding ratio (VHR) characteristics so that liquid crystals with low resistivity could provide higher VHRs compared with the twisted nematic effect. This experimental result was obtained when electric fields were applied approximately parallel to the substrate plane using the IPS electro-optical effect. We found that the in-plane electric field generates supplementary capacities which support retention of an externally applied voltage over the liquid crystal layer during non-selected periods of the active matrix driving scheme, because the liquid crystal layer can be connected with an insulating layer, an orientation layer and even a substrate in parallel. Based on these advantageous VHR characteristics, liquid crystal materials suitable for the IPS effect were appropriately optimized. We propose evaluation parameters, derived from the physical switching principles of the liquid crystals, to obtain lower driving voltage and faster response speeds. These parameters are effective in optimizing the physical properties of liquid crystals without variation of the cell gap. We use the proposed evaluation parameters and the advantageous VHR characteristics to demonstrate the optimization approach and we suggest a novel possible use of liquid crystal materials with low resistivity which cannot be implemented conventionally. Finally, we prove that liquid crystals with low resistivity generate the Ir internal potential by the drift of ionic species.

1. Introduction

The development of in-plane switching (IPS) electro-optical liquid crystal displays (LCDs) combined with an active matrix driving technique in thin film transistors (TFTs) has greatly advanced LCD technology, because the severe viewing angle problems of the LCDs were overcome [1–5]. Interdigital electrodes were originally used in the investigation of acoustic surface waves [6–8], integrated optics [9] and electro-optics [10]. The first application of interdigital electrodes to liquid crystals was to combine them with the dynamic scattering electro-optical effect [11]. Soref [12] extended this work and investigated three new electro-optical effects of liquid crystal reorientation using transparent indium tin oxide interdigital electrode arrays. Homeotropic, homogeneous and twisted liquid crystal orientations with positive dielectric anisotropy were demonstrated using interdigital electrodes in two tunable birefringence effects and in a tunable optically rotatory effect. Field distributions were discussed regarding the point that field lines between the electrodes are nearly parallel to the plane of the substrates and the fields distribute perpendicularly with respect to the substrate surface near and above the electrodes. Principles of each electro-optical effect were described qualitatively and the deformation threshold of the liquid crystal orientation was empirically analysed. However, detailed analyses and investigations regarding electro-optical effects using interdigital electrodes have not been reported since then, because the twisted nematic (TN) effect [13] was put to practical use and no further attention was paid to interdigital electrode arrays.

In spite of the widely suitable TN effect, some problems remained including that this effect shows narrow and limited viewing angle characteristics. To improve grey scale reversal and to decrease contrast ratio and colour shifts from oblique directions with respect to the substrate plane, efforts have been made using optical compensation with retardation films [14–18], multidomain methods [19–32] and the optically compensated controllable effect [33–35]. Baur's group, however, predicted from computer simulations that the in-plane switching of liquid crystals with interdigital electrodes, which has been neglected for a long time, could provide extremely

* Author for correspondence. Present address: Electron Tube & Devices Division, Hitachi, Ltd, 3300 Hayano, Mobara-shi, Chiba-ken 297, Japan; e-mail: mooe@cm.mobara.hitachi.co.jp.

0267–8292/98 $12.00

wide viewing angle characteristics [36]. We also investigated this technology combined with the drastic change of electrode arrangement with conventional TFTs at around the same time [1, 2]. In order to develop liquid crystal materials suitably applicable to the IPS electro-optical effect with active matrix driving techniques, we analysed the physical switching principles of liquid crystals driven by an in-plane electric field, i.e. threshold behaviour [1, 37, 38], response mechanism [38, 39], pre-tilt angle-dependent viewing angle characteristics [40], switching of negative and positive dielectro-anisotropic liquid crystals [41], and the quantatively analysed margin of the cell gap to ensure uniform optical properties [42].

Although many substances and mixtures of liquid crystals have been developed based on property requirements for the use of TFT applications, a large electrical resistivity of these materials was a necessary condition for the voltage-holding ratio (VHR) characteristic to be high [43–47]. Only in divided time periods are the signals driving the liquid crystals addressed, so the liquid crystals must store the provided charge and hold the supplied voltage during non-selected periods. Basically, the function of the TFTs formed on LCDs is to control the transmittance of each pixel by charging the capacities between pixels and ground electrodes through gate and bus lines. It is well known that the resistivity of the liquid crystals governs the VHR characteristics: the lower the resistivity of the liquid crystals, the lower the VHRs. The relaxation time of the discharging process over the liquid crystal layer can be basically described by the mathematical product of the resistance and capacity of the liquid crystals in the conventional TN electro-optical effect driven by TFTs. This description corresponds to the fact that liquid crystal materials used in the conventional TN effect with a TFT driving scheme have been limited by their resistivity. Terminally fluorinated liquid crystal substances and their mixtures have been developed to meet such a requirement that the resistivity is stably high so as to keep higher VHRs [48–52].

On the other hand, it is important to understand what physical properties of liquid crystals are required so as to optimize the performance of the IPS electro-optical effect driven by TFTs. Knowledge about optimization developed for the conventional TN effect driven by TFTs, cannot be simply applied to the IPS electro-optical effect, because the parameters affecting the performance of the IPS effect are more complicated than those of the TN effect. In particular, the threshold voltage in the IPS effect (which is the most important characteristic when optimizing liquid crystal materials) is influenced by the initial orientation direction of the liquid crystals [53, 54], the width of the interdigital electrodes [55, 56], the cell gap and the distance between two interdigital electrodes, in addition to the dielectric and elastic properties of liquid crystal materials [37, 38]. Therefore, it is essential to establish a new optimization approach for liquid crystals taking into account the physical switching behaviour of the IPS effect.

In this article, we report the use of a novel concept to obtain liquid crystal materials applicable to the IPS electro-optical effect. First, we describe the unusual VHR characteristics when using the IPS effect. These lead to the noteworthy possibility that liquid crystals which are not applicable to the conventional active matrix driving scheme due to the restriction of their resistivity, may in fact be used in the case of the IPS effect. Second, we introduce evaluation parameters to optimize liquid crystal materials for use of the IPS effect, where the parameters to be optimized are more complicated in comparison with the TN effect. Finally, we demonstrate the optimization concept for liquid crystals using the IPS effect by employing the proposed evaluation parameters and the novel VHR characteristics.

2. Experimental

2.1. *Measurements*

Figure 1 (*a*) illustrates the circuit diagram for measuring the VHR characteristics. Either Sw1 or Sw2 was connected to the circuit during the selected periods, while neither Sw1 nor Sw2 was connected during the nonselected periods. The VHRs were obtained by measuring the profiles of the voltage, which was applied to the liquid crystals in selected periods, during nonselected periods. The schematic waveform applied to the liquid crystals and the definition of the VHR obtained by the relaxation of the liquid crystals during nonselected periods are given in figure 1 (*b*). The VHR was defined as the ratio, V/V_0, of the initially applied voltage (V_0) and the finally obtained voltage when relaxed during the nonselected period (V).

For the measurements of voltage-dependent transmittance, a polarizing microscope (Olympus BH-3) with a filter for brightness correction and a photomultiplier were used as illustrated in figure 2 (*a*). Light transmitted through samples was detected with the photomultiplier as the desired voltage was applied to the samples. The polarizer and the analyser were always set at right angles to the axes with the polarization axis of the polarizer being in good agreement with the rubbing direction. Figure 2 (*b*) defines the arrangement of the polarizer, the analyser and the rubbing direction. The polarizer, set on the side of the incident light, and the analyser, set on the side of the outgoing light, are represented as P1 and P2, respectively.

Response times of the liquid crystals were measured from their optical signals triggered by switching a wave generator (Hewlett-Packard 8175A) on and off. The signals from the liquid crystal cells were observed with

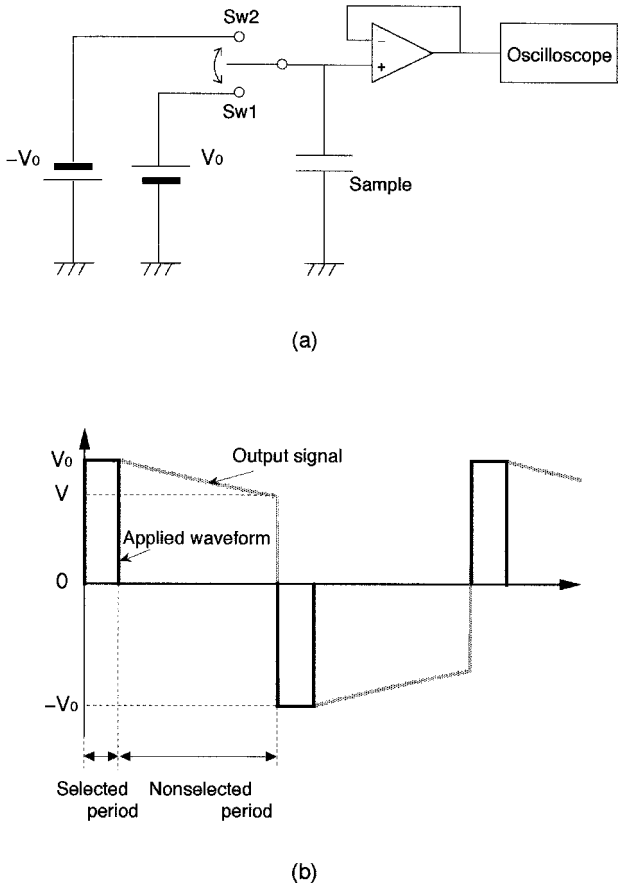

Figure 1. (*a*) Circuit diagram of the measurement system for VHR characteristics. (*b*) Schematic waveform applied to liquid crystals and a corresponding output signal for the measurements of VHR characteristics.

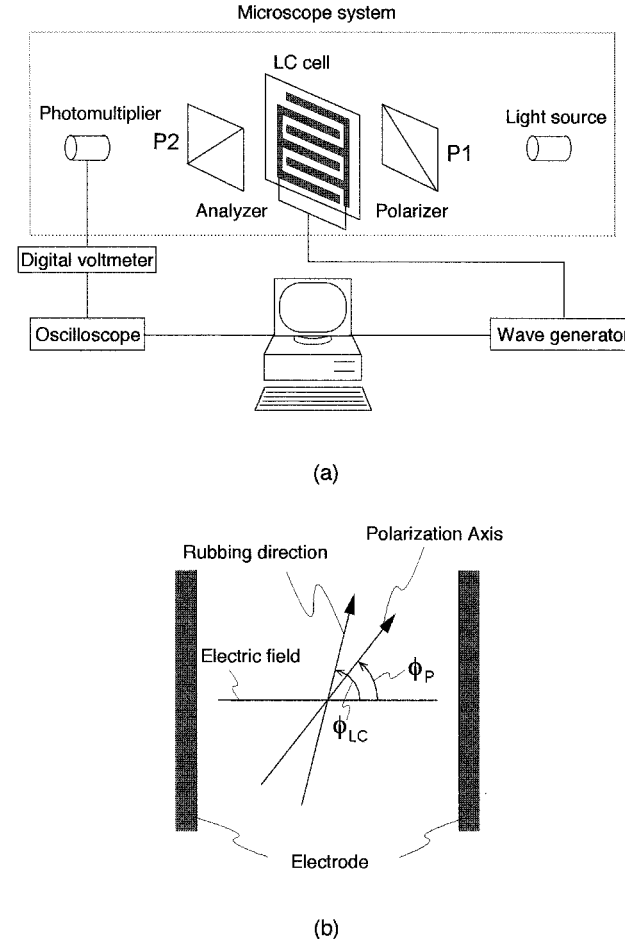

Figure 2. (*a*) Diagram of the measurement of voltage-dependent transmittance and response times. (*b*) Definition of the polarization axes of the polarizer and analyser and the rubbing direction. ϕ_P represents the angle of the polarization axis of the polariser or analyser. When identifying the polarizer, ϕ_P is replaced by ϕ_{P_1}; ϕ_{P_2} is used for the analyser.

a digital oscilloscope (Hewlett-Packard 54110A). The switching-on and -off times (T_{on} and T_{off}) were defined as the times from the moment of the field-on and -off to that at which a 90% optical change from the off-state to the on-state or vice versa is achieved.

2.2. *Sample preparations and materials*

For the IPS cells, chromium interdigital electrodes, whose width was set to 10 μm, were prepared on one substrate and no electrodes were formed on the other, while a pair of the substrates had transparent indium tin oxide electrodes on each substrate surface for the TN cells. A pair of substrates for the IPS was set in the same rubbing direction to obtain homogeneously aligned liquid crystals. For spacers, the desired size polymer beads were scattered over the lower substrate to provide a uniform cell gap.

As liquid crystal materials for the analysis of VHR characteristics, a fluorinated mixture, MLC-6252 (Merck Japan) was used as base liquid crystal mixture and cyano-substances were added to it to decrease the resistivity for the voltage-holding ratio measurements. The physical properties of these liquid crystals are as follows: MLC-6252 (nematic–isotropic temperature, T_{NI}: 63°C; birefringence, Δn: 0.0865 (20°C); dielectric anisotropy, $\Delta\varepsilon$: 14.8 (20°C, 1 kHz); viscosity, η: 26 cp (20°C)). The resistivity was systematically varied by doping MLC-6252 with 1-(4-cyanophenyl)-4-propylcyclohexane, 1-(4-cyanophenyl)-4-pentylcyclohexane and 4-cyano-1-(4-ethylbenzoyloxy)-3-fluorobenzene.

For the orientation layer, RN-718 (Nissan Chemical Industries, Ltd.) and PIQ-5300 (Hitachi Chemical Co, Ltd.) were used without further purification.

3. Results and discussion

3.1. *Voltage-holding ratio (VHR) characteristics*

The electrical characteristics of liquid crystal cells are substantially influenced by the cell structures. To clarify differences in electrical characteristics between

the IPS and conventional TN effects, equivalent circuits corresponding to each cell structure were employed. Figure 3 compares the equivalent circuit models for the IPS and TN cell structures, taking into account the electric field directions and cross-sectional structures for each effect. For the TN effect, a resistance–capacity network corresponding to the liquid crystal layer is connected with other resistance–capacity components to make up an insulating layer and/or an orientation layer in series. By contrast, the in-plane electric field of the IPS effect provides a parallel connection of resistance–capacity networks, corresponding to an insulating layer, an orientation layer and/or even a substrate, with the liquid crystal layer. Therefore, different electrical characteristics between the IPS and TN effects were predicted to be generated due to the difference in the electrical connection of the liquid crystal layer with other components.

Figure 4 compares the VHR signal observations between the IPS and the conventional TN effects using the same materials for liquid crystals and orientation layers. In the IPS effect better VHR characteristics were obtained both for the liquid crystals with low resistivity and for the PIQ orientation layer—typical conditions under which VHR characteristics deteriorate in the TN effect. The resistivity of the liquid crystals was slightly different due to experimental errors. However, the VHR characteristics using the IPS effect were presumably good in spite of the lower resistivity of the liquid crystals being used, compared with the TN effect. Figure 5 compares the temperature-dependent VHR characteristics between the IPS and TN effects. The IPS effect showed more stable characteristics compared with the TN effect over the temperature range in spite of the same liquid crystal material being used. Basically, a higher temperature decreases the viscosity of the medium and results in lower resistivity of the liquid crystals, causing deterioration of the VHR characteristics. Therefore, the results shown in figure 5 suggest that VHR characteristics seem to be insensitive to the resistivity of the liquid crystal medium.

Figure 6 compares the dependence of VHR characteristics on the resistivity of the liquid crystals between the IPS and TN effects, with the resistivity of the liquid crystals being systematically varied. Lower resistivity of the liquid crystals reduced VHR characteristics in the TN effect, while they were relatively constant in the IPS effect. For the PIQ orientation layer, the VHR was extremely low regardless of the high resistivity of the liquid crystals in the TN effect. However, the IPS effect offered much better VHR characteristics for the same

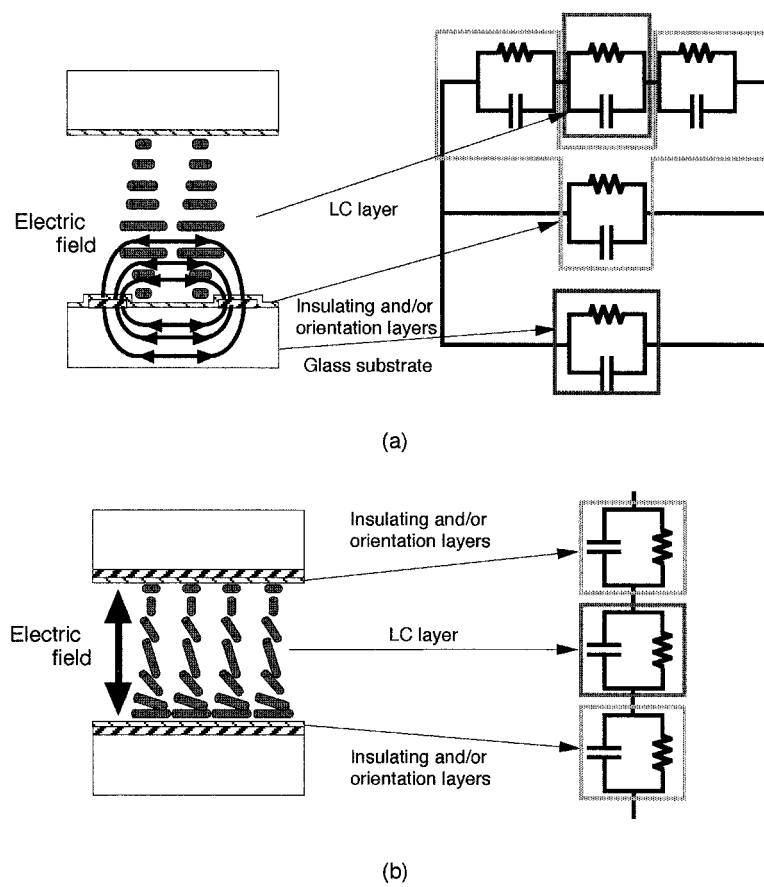

Figure 3. Equivalent circuit models (*a*) for the IPS cell structure and (*b*) for the TN cell structure.

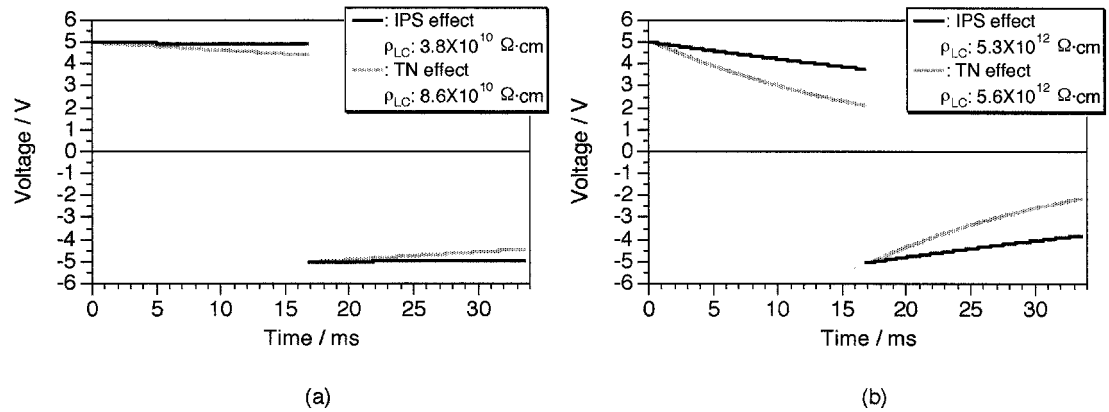

Figure 4. VHR signals for the IPS and TN effects. (*a*) LC: MLC-6252 doped with 15% 1-(4-cyanophenyl)-4-propylcyclohexane, 15% 1-(4-cyanophenyl)-4-pentylcyclohexane and 15% 4-cyano-1-(4-ethylbenzoyloxy)-3-fluorobenzene, orientation layer: RN-718. (*b*) LC: MLC-6252 doped with 15% 1-(4-cyanophenyl)-4-propylcyclohexane and 15% 1-(4-cyanophenyl)-4-pentylcyclohexane, orientation layer: PIQ-5300.

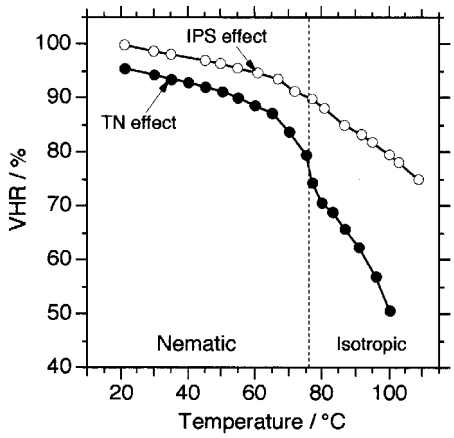

Figure 5. Temperature-dependent VHR characteristics for the IPS and TN effects. The liquid crystal (nematic–isotropic transition temperature $T_{NI} = 76.1°C$) used in the experiments was MLC-6252 doped with 15% 1-(4-cyanophenyl)-4-propylcyclohexane and 15% 1-(4-cyanophenyl)-4-pentylcyclohexane. The orientation layer was RN-718. The non-selected period was set to 16.7 ms.

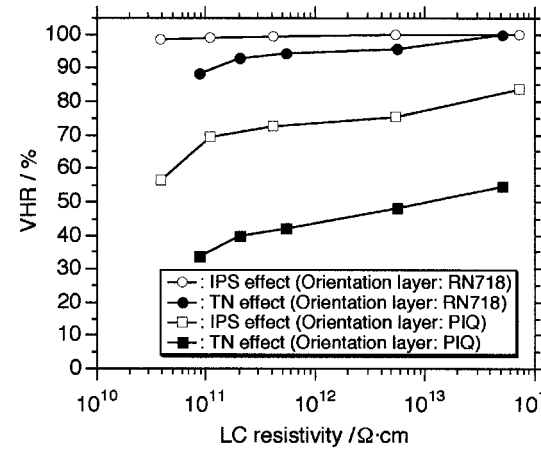

Figure 6. Relationship between VHR characteristics and the resistivity of liquid crystals using the IPS and TN effects. The resistivities of the liquid crystals used were varied by doping MLC-6252 with 1-(4-cyanophenyl)-4-propylcyclohexane, 1-(4-cyanophenyl)-4-pentylcyclohexane and 4-cyano-1-(4-ethylbenzoyloxy)-3-fluorobenzene.

materials. The difference in the VHR characteristics between the IPS and TN effects was the degree of the sensitivity to the resistivity of the liquid crystals: the VHR was less sensitive to the resistivity of the liquid crystals when using the IPS effect. These results suggested the discharging process over the liquid crystal layer differed between the effects, and an explanation of this mechanism must be closely related to the electrically working components involved in each liquid crystal cell structure.

As was predicted from the equivalent circuit models for the IPS and TN cell structures shown in figure 3, these unusual features of the VHR characteristics using the IPS effect can be understood by comparing the components of the liquid crystal cell for equivalent circuits when discussing phenomena related to the electrical process. For the case when the electric field is applied along a direction perpendicular to the substrate plane, the voltage decay process over the liquid crystal layer in relation to time (t) during the nonselected periods can be approximately described, with an assumption of a single discharge process, as follows:

$$\frac{V}{V_0} = \exp\left(-\frac{t}{C_{LC}R_{LC}}\right) = \exp\left(-\frac{t}{\varepsilon_{LC}\rho_{LC}}\right) \quad (1)$$

where C_{LC}, R_{LC}, ε_{LC} and ρ_{LC} are the capacity, the resistance, the dielectric constant and the resistivity of liquid crystals, respectively. This description corresponds to an equivalent circuit of resistance and capacity components of the liquid crystal. Therefore, it should be

noted that the smaller the resistivity of the liquid crystals, the lower the VHR characteristics, because the relaxation time, which corresponds to the mathematical product of the capacity and resistance of the liquid crystals, becomes smaller. However, not only the resistivity of the liquid crystals but also other factors, e.g. their surface interaction with the orientation layer, the polarity and dielectric properties of the orientation layers, etc., are relevant to the VHR characteristics.

When considering the electrically parallel connection of the liquid crystals with the orientation and insulating layers and substrates, it is necessary to discuss why the VHR characteristics are relatively insensitive to the resistivity of the liquid crystals when using the IPS effect. Two mechanisms are possible. One is the case that supplementary resistance (R_{SUPPL}) is much smaller than the resistance of the liquid crystal layer (R_{LC}), where the supplementary resistance involves all resistances connected with the liquid crystal layer in parallel, i.e. the composite resistance of the orientation, the insulating layers and the substrates. When $R_{LC} \gg R_{SUPPL}$, R_{SUPPL} can dominate the relaxation of the charges over the liquid crystal layer during the nonselected periods. However, the experimentally obtained resistance of the IPS cell not filled with liquid crystals was larger than 100 GΩ, which was enough to retain whole charges in the nonselected periods; therefore, this hypothesis may not be valid. In the second mechanism, supplementary capacity functions as a support to retention of the charges over the liquid crystal layer. The supplementary capacity is composed of the effects of orientation, the insulating layers and the substrates, and seems to act as an additional capacity for the liquid crystals. Furthermore, the capacity corresponding to the liquid crystal layer in the IPS effect is smaller than that in the TN effect so that even a small supplementary capacity can effectively contribute to supporting the retention of the charges in the liquid crystal layer. The capacity of the experimentally used IPS cell without liquid crystals was around 40 pF.

Figure 7 shows the calculated results for VHRs as a function of the resistance of the liquid crystals and varied with supplementary capacities which are assumed to be connected with the liquid crystal layer in parallel. The calculations simulated the behaviour of the VHR characteristics well and demonstrated the support in retention of the voltage over the liquid crystal layer. Figure 8 compares temperature-dependent VHRs for electrode distances of 15 and 30 μm. The larger electrode distance led to a more effective in-plane electric field in comparison with the field component perpendicular to the substrates. This result also confirmed that the electric field parallel to the substrate plane caused the advantageous behaviour of the VHR characteristics.

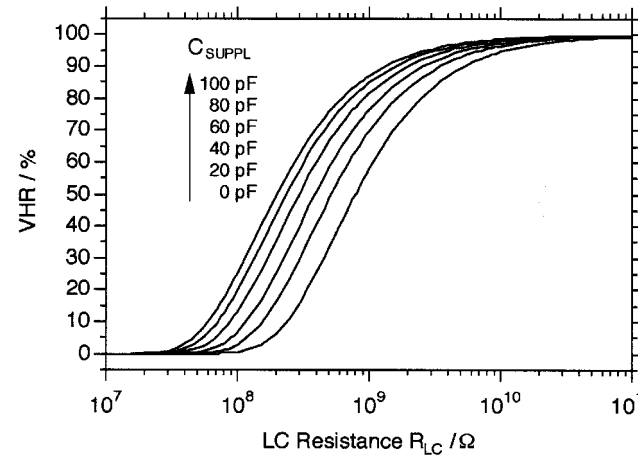

Figure 7. Simulation of the effect of supplementary capacities on the VHRs as a function of liquid crystal resistivity in the IPS effect.

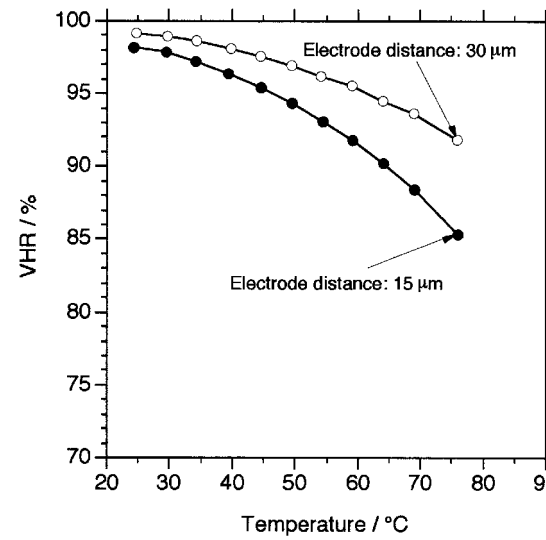

Figure 8. The influence of electrode distance on temperature-dependent VHRs in the IPS effect.

3.2. *Optimization concept for liquid crystal properties*

Liquid crystal materials for the IPS effect may be suitably optimized by considering complicated parameters of the physical switching principles, which result from application of the electric field parallel to the substrate plane. The differences in the switching of the liquid crystals in relation to the IPS and TN effects arise intrinsically from the relation of the electric field with the liquid crystal layer normal direction. The IPS effect provides four additional parameters affecting the threshold behaviour of the liquid crystal in comparison with the TN effect, i.e. the thickness of liquid crystal layer (the cell gap), the distance between neighbouring interdigital electrodes, the width of each electrode and the initial orientation of the liquid crystal, corresponding to the

rubbing direction. The threshold voltage (V_{th}) is well understood by the following expression which is derived using one dimensional analysis with the assumption that the electric field is uniform in the liquid crystal layer [37, 38]:

$$V_{th}^{IPS} = E_{th} \times \ell = \frac{\pi \ell}{d}\left(\frac{K_{IPS}}{\varepsilon_0 |\Delta\varepsilon|}\right)^{1/2} \quad (2)$$

where $\mathbf{E}_{th}$ is the threshold electric field for the liquid crystals being driven, ℓ is the electrode distance from edge to edge, d is the cell gap, K_{IPS} is the elastic constant for the IPS effect contributed by the combination of splay, twist and bend deformations in actual switching, ε_0 is the vacuum dielectric constant and $\Delta\varepsilon$ is the dielectric anisotropy. K_{IPS} should correspond not to K_2 but to $\alpha K_1 + \beta K_2 + \gamma K_3$ (a linear combination of splay, twist and bend elastic constants), because the actual deformation of liquid crystals is affected by the deformed electric field near the edges of the electrodes [41]. Equation (2) indicates that the threshold characteristic of the liquid crystals is directly governed by the electric field strength, because the electrode distance is independent of the cell gap and V_{th}^{IPS} is a function of the cell gap and the electrode distance: $V_{th}^{IPS} = f(d, \ell)$. In the case of the TN effect, however, the threshold voltage is described as follows [13, 57, 58]:

$$V_{th}^{TN} = \mathbf{E}_{th} \times d = \pi\left[\frac{K_1 + (K_3 - 2K_2)/4}{\varepsilon_0 \Delta\varepsilon}\right]^{1/2}. \quad (3)$$

The electrode distance is always identified with the cell gap in the effects in which the electric field is applied along the direction perpendicular to the substrates such as the TN effect. This means that V_{th}^{TN} is neither a function of the cell gap nor the electrode distance. In this way, a difference exists in the threshold voltage between the effects in which the electric field is applied along the directions parallel or perpendicular to the substrate plane. In the IPS effect, the threshold voltage is strongly influenced by the cell gap, and precise control of the cell gap is required to obtain a uniform display. A larger cell gap and smaller electrode distance are preferable for obtaining a lower threshold voltage; however, the former results in a slower response speed of the liquid crystals and the latter is irrelevant to the dynamical response times [39]. The threshold voltage is also affected by the electrode width when the width is on the same order as the cell gap, or smaller, because the electric field distribution is varied by a change of the electrode width [55, 56].

Before optimizing the liquid crystal properties suitable for IPS switching, the initial orientation direction of the liquid crystals corresponding to the rubbing direction has to be considered. Figure 9 shows the influence of the rubbing direction on the driving voltages and the response

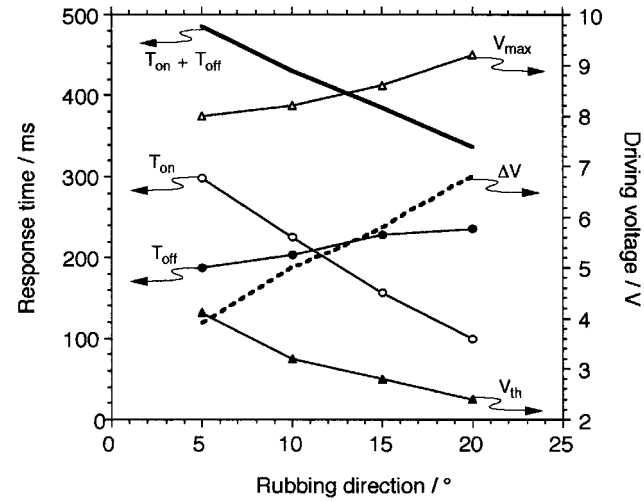

Figure 9. Dependence of the rubbing direction on driving voltages and response times. (*a*) LC: ZLI-2806, (*b*) LC: ZLI-4535.

times. Here the driving voltages involve the operating voltage (V_{max}) which gives maximum transmittance, the threshold voltage (V_{th}) which gives a transmittance change of 1% from the minimum state, and the width of the driving voltage (ΔV) corresponding to the difference between the operating voltage and the threshold voltage. The responding axes are different by 90° between negative (Nn) and positive (Np) dielectrically anisotropic liquid crystals like ZLI-2806 and ZLI-4535 as shown in figures 9(*a*) and 9(*b*). Regardless of the polarity of the dielectric anisotropy, ΔV became larger by the amount of the increased V_{max} and the decreased V_{th}, as the angle

of the rubbing direction (ϕ_{LC}) is increased. The fact that V_{th} is influenced by ϕ_{LC} can be explained by the dielectric torque Γ in the liquid crystal medium given by

$$\begin{aligned}\Gamma &= |\Delta\varepsilon(\mathbf{n}\ \mathbf{E})\mathbf{n}\times\mathbf{E}| \\ &= \left|\Delta\varepsilon\mathbf{E}^2\sin\left(\frac{\pi}{2}-\phi_{LC}\right)\cos\left(\frac{\pi}{2}-\phi_{LC}\right)\right| \\ &= |\Delta\varepsilon|\mathbf{E}^2\sin\phi_{LC}\cos\phi_{LC} \qquad (4)\end{aligned}$$

where $\mathbf{n}$ is the liquid crystal director and $\mathbf{E}$ is the electric field. Therefore, the decrease of V_{th} by the larger ϕ_{LC} could be due to the larger torque of the electric field. However, experimental results revealed that optical changes took place quickly when V_{th} increased, due to the smaller ϕ_{LC}. With regard to response times, the switching-on time was reduced (while the operating voltage increased) as ϕ_{LC} changed from smaller to larger angles. However, the switching-off times were relatively insensitive to ϕ_{LC} because the elastic torque just restored the initial state from the 45° twisted state. With a view to optimizing the driving voltage and the response times, a trade-off relationship existed between ΔV and $T_{on}+T_{off}$. However, well-balanced switching-on and -off times should be seen when ϕ_{LC} is 15° in the case of Nn type liquid crystal and 105° in the case of Np type liquid crystal. Therefore, the rubbing directions were set to 15° and 105° for the Nn and Np type liquid crystals, respectively, in the following work.

With constant rubbing direction and electrode width, evaluation parameters for the liquid crystal materials can be proposed so as to optimize the properties for the threshold voltage and response time. To reduce the influence of the variation of the cell gap on the threshold voltage, a driving voltage parameter (DVP or DVP') can be made, i.e. the threshold voltage multiplied by the cell gap, or, in addition, divided by the electrode distance given as [37, 38]

$$DVP = V_{th}^{IPS}\times d = \pi\ell\left(\frac{K_{IPS}}{\varepsilon_0|\Delta\varepsilon|}\right)^{1/2},$$

or

$$DVP' = V_{th}^{IPS}\times\frac{d}{\ell} = \pi\left(\frac{K_{IPS}}{\varepsilon_0|\Delta\varepsilon|}\right)^{1/2}. \qquad (5)$$

A response parameter (RP) can be introduced, without the influence of the cell gap and the electric field by [38, 39]

$$RP = \frac{T_{eff}}{d^2}\propto\frac{\gamma_1}{\pi^2 K_{IPS}}. \qquad (6)$$

The switching-on time is strongly dependent on the electric field strength, while the switching-off time can be affected by the cell gap despite the independence of the electric field. Therefore, the switching-off time divided by the square of the cell gap can be the response parameter to evaluate the intrinsic response capability of liquid crystal materials without variation of the cell gap.

By using these two parameters, the evaluation of the liquid crystals for driving voltage and response time can be carried out precisely, because these parameters are composed only of the physical properties of liquid crystals. Figure 10 shows an experimentally obtained plot of the evaluation parameters for liquid crystal mixtures consisting of terminally fluorinated liquid crystal substances, i.e. 3, 4-difluorobenzene and 3, 4, 5trifluoro-benzene derivatives, which were developed for the conventional active matrix driving scheme. The driving and response characteristics showed the trade-off relationship through the elasticity of the liquid crystals, as was predicted from the driving and response parameters, DVP' and RP. The relationship between the driving and response parameters, DVP' and RP, can be obtained using equations (5) and (6):

$$DVP' = \left(\frac{\gamma_1}{\varepsilon_0|\Delta\varepsilon|}\times\frac{1}{RP}\right)^{1/2}. \qquad (7)$$

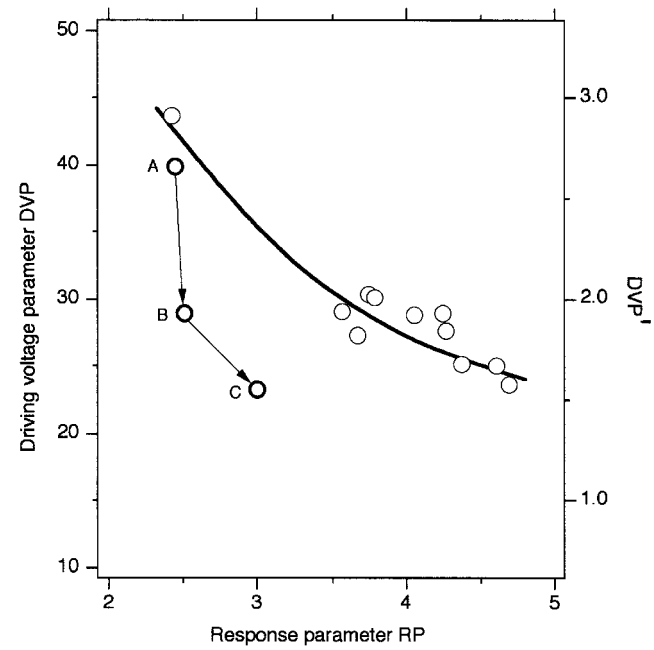

Figure 10. Plot of evaluation parameters for some liquid crystal materials, and results of doping liquid crystal mixtures with a cyano-substance. A is MLC-6252; B is MLC-6252 doped with 15% 1-(4-cyanophenyl)-4-propylcyclohexane and 15% 1-(4-cyanophenyl)-4-pentylcyclohexane; C is the further addition of 10% 4-cyano-1-(4-ethylbenzoyloxy)-3-fluorobenzene to mixture B. Others are mixtures composed of 3, 4-difluorobenzene and 3, 4, 5-trifluorobenzene derivatives. The interdigital electrode distance is 15 μm; $\phi_{LC}=105°$, $\phi_{P_1}=105°$, $\phi_{P_2}=15°$.

The difficulty is in the trade-off relationship between the driving voltage and response parameters, DVP' and RP, when the ratio of the twist viscous coefficient, γ_1, to the dielectric anisotropy, $\Delta\varepsilon$, does not change drastically. A small twist viscous coefficient, γ_1, with large dielectric anisotropy, $\Delta\varepsilon$, can be effective in overcoming the trade-off relationship between DVP' and RP so that DVP' decreases while keeping a certain smaller RP. The solid line in figure 10 shows the trade-off relationship between DVP' and RP, which is formed by mixtures containing terminally fluorinated liquid crystals, i.e. 3, 4-difluorobenzene and 3, 4, 5-trifluorobenzene derivatives. However, terminally cyano-substituted substances proved to be more effective in getting a breakthrough in the trade-off relationship so that it was possible to approach the parameter region which corresponded to a much lower driving voltage while maintaining the faster response time. The terminally cyano-substituted substances showed smaller twist viscous coefficient with larger dielectric anisotropy.

3.3. *Advantageous characteristics of liquid crystals with low resistivity*

Cyano-substances show relatively lower resistivity due to the large dipole moment of the cyano substituent. Locally polar properties induced by the cyano substituent are prone to dissolve impure ionic species. Therefore, the doping of cyano-substances into liquid crystal mixtures decreases the resistivity of the liquid crystals. This design concept has not been accepted for the conventional TN effect with the active matrix driving technique, because liquid crystals with low resistivity reduce the VHR characteristics. Although high VHRs can be maintained while employing liquid crystals with low resistivity in the IPS effect, the ionic flow induced by the electric field in the liquid crystal layer should be measured to evaluate the effect of the low resistivity of the liquid crystals. A parameter for ionic flow can be introduced, assuming the d.c. is applied to the liquid crystals in addition to a rectangle-like and non-biased a.c. waveform. Nematic liquid crystals respond to the root mean square of the voltage. The ionic flow generates an internal field in the liquid crystal layer, because the ionic species move so as to reduce the externally applied electric field. Therefore, the internal potential (V_{PI}) caused by the drift of the ionic species can be described as

$$V_{PI} = V_{rms} - V_{a.c.} = \left(\frac{\int_0^T V_{ext}^2 \, dt}{T} \right)^{1/2} - V_{a.c.}$$

$$= (V_{a.c.}^2 + V_{d.c.}^2)^{1/2} - V_{a.c.} \qquad (8)$$

where V_{rms} is the root mean square of the voltage, $V_{a.c.}$ is the non-biased a.c. voltage and $V_{d.c.}$ is the d.c. voltage. Figure 11 ccompares the experimental and calculated results on the generation of the internal potential between liquid crystals with high and low resistivities. With the higher resistivity liquid crystals, the calculated line was not in good agreement with the experimentally obtained results: no internal potential therefore occurred. In contrast, the lower resistivity liquid crystals did give rise to internal potentials while applying the biased d.c. voltage, since experimental results coincided with those calculated. These results suggest that liquid crystals with low resistivity could cancel the d.c. voltage while showing higher VHRs using the IPS effect, in comparison with the case in which the electric field was applied perpendicular to the substrate plane.

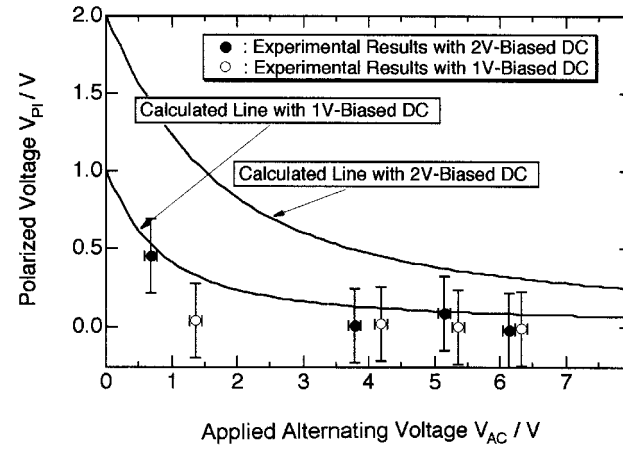

(a)

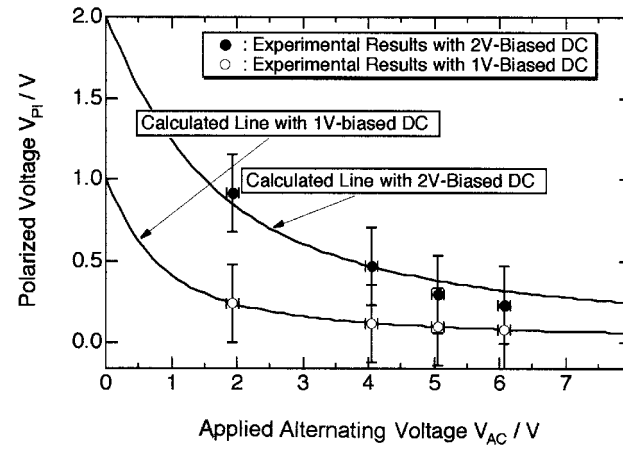

(b)

Figure 11. Generation of the internal potential V_{PI} using liquid crystals with high and low resistivity. (*a*) $\rho_{LC} = 2.0 \times 10^{13}\ \Omega$ cm, (*b*) $\rho_{LC} = 5.0 \times 10^{10}\ \Omega$ cm.

4. Conclusions

We propose the optimization concept for liquid crystal materials suitable for the IPS electro-optical effect. Conventional liquid crystal mixtures composed of only fluorinated substances, so as to keep higher VHRs, could not meet the requirements for lower threshold and faster response speeds in the IPS effect. The key was in finding unusual behaviour of VHR characteristics using the IPS effect, i.e. even when employing liquid crystals with much lower resistivity than is applicable to the conventional active matrix driving technique, the VHRs were higher than those using conventional electric fields applied perpendicular to the substrate plane. We concluded that the in-plane electric field generated supplementary capacitances to support the retention of an externally applied voltage over the liquid crystal layer during non-selected periods of the active matrix driving scheme, because the liquid crystal layer could be connected with an insulating layer, an orientation layer and even a substrate in parallel.

We also clarified the effects of rubbing direction-dependent driving voltages and response times. The width of driving voltage, ΔV, became larger and the response time, $T_{on} + T_{off}$, smaller, as the angle of the rubbing direction, ϕ_{LC}, increased. Then, evaluation parameters were proposed for optimization of the driving voltage and response time, which are effective in evaluating the physical properties of liquid crystals so that they are unaffected by the variation of cell gap. The relationship between the threshold and response characteristics proved to be a trade-off with elastic properties of the liquid crystals. However, cyano-substances could decrease the threshold voltage effectively while keeping low viscosity, so that the threshold became lower while maintaining a faster response time. The lower resistivity caused by doping with cyano-substances produced advantageous VHR characteristics when using the IPS effect, as was explained above. Furthermore, the internal potential in the liquid crystals was evaluated when a biased d.c. voltage was applied; low resistivity materials had the ability to generate an internal potential large enough to cancel the d.c. voltage in the liquid crystals.

We wish to thank M. Ohta for his research into designing electrode arrays and driving methods for the IPS effect. Gratitude is also extended to H. Kawakami, K. Kinugawa, T. Futami and N. Konishi of the Electron Tube & Devices Division of Hitachi, Ltd for their support of this research.

References

[1] Oh-E, M., Ohta, M., Aratani, S., and Kondo, K., 1995, in Proceedings of the 15th International Display Research Conference (SID, Hamamatsu, 1995), p. 577.

[2] Ohta, M., Oh-E, M., and Kondo, K., 1995, in Proceedings of the 15th International Display Research Conference (SID, Hamamatsu, 1995), p. 707.

[3] Kondo, K., Konishi, N., Kinugawa, K., and Kawakami, H., 1995, in Proceedings of the 2nd International Display Workshop, Vol. 2 (SID, Hamamatsu, 1995), p. 43.

[4] Ohta, M., Kondo, K., and Oh-E, M., 1996, *IEICE Trans. Electron*, **E79-C,** 1069.

[5] Kondo, K., Kinugawa, K., Konishi, N., and Kawakami, H., 1996, *Dig. Tech. Pap.*, SID International Symposium, San Diego, 1996, p. 81.

[6] White, R. M., and Voltmer, F. W., 1965, *Appl. Phys. Lett.*, **7,** 314.

[7] Bahr, A. J., Lee, R. E., and Podell, A. F., 1972, *Proc. IEEE.*, **60,** 443.

[8] Mortley, W. S., 1973, *Proc. IEEE*, **61,** 133.

[9] Polky, J. N., and Harris, J. H., 1972, *Appl. Phys. Lett.*, **21,** 307.

[10] Wu, S. Y., Takei, W. J., and Francombe, M. H., 1973, *Appl. Phys. Lett.*, **22,** 26.

[11] Kobayashi, S., Shimojo, T., Kasano, K., and Tsunda, I., 1972, *Dig. Tech. Pap.*, SID International Symposium, New York, 1972, p. 68.

[12] Soref, R. A., 1974, *J. appl. Phys.,* **45,** 5466.

[13] Schadt, M., and Helfrich, W., 1971, *Appl. Phys. Lett.*, **18,** 127.

[14] Yamagishi, N., Watanabe, H., and Yokoyama, K., 1989, in Proceedings of the 9th International Display Research Conference (SID, Kyoto, 1989), p. 316.

[15] Ong, H. L., 1992, in Proceedings of the 12th International Display Research Conference (SID, Horoshima, 1992), p. 247.

[16] Eblen, J. P. Jr., Gunning, W. J., Beedy, J., Taber, D., Hale, L., Yeh, P., and Khoshnevisan, M., 1994, *Dig. Tech. Pap.*, SID International Symposium, San Jose, 1994, p. 245.

[17] Mukai, J., Mazaki, H., Satoh, Y., Kobori, Y., Toyooka, T., and Itoh, H., 1995, in Proceedings of the 15th International Display Research Conference (SID and Institute of Television Engineers of Japan, Hamamatsu, 1995), p. 949.

[18] Mori, H., Itoh, Y., Nishiura, Y., Nakamura, T., and Shinagawa, Y., 1996, in Proceedings of the 3rd International Display Workshop (SID, Kobe, 1996), p. 189.

[19] Yang, K. H., 1991, in Proceedings of the 11th International Display Research Conference (SID, San Diego, 1991), p. 68.

[20] Koike, Y., Kamada, T., Okamoto, K., Ohashi, M., Tomita, I., and Okabe, M., 1992, *Dig. Tech. Pap.*, SID International Symposium, Boston, 1992, p. 798.

[21] Takatori, K., Sumiyoshi, K., Hirai, Y., and Kaneko, S., 1992, in Proceedings of the 12th International Display Research Conference (SID, Horoshima, 1992), p. 591.

[22] Lien, A., and John, R. A., 1993, *Dig. Tech. Pap.*, SID International Symposium, Seattle, 1993, p. 269.

[23] Toko, Y., Sugiyama, T., Katoh, K., Iimura, Y., and Kobayashi, S., 1993, *J. Appl. Phys.*, **74,** 2071.

[24] Takatori, K., and Sumiyoshi, K., 1995, *Mol. Cryst. liq. Cryst.*, **263,** 445.

[25] Yamada, N., Kohzaki, S., Fukuda, F., and Awane, K., 1995, *Dig. Tech. Pap.*, SID International Symposium, Orlando, 1995, p. 575.

[26] Chen, J., Bos, P. J., Bryant, D. R., Johnson, D. L., Jamal, S. H., and Kelly, J. R., 1995, *Dig. Tech. Pap.*, SID International Symposium, Orlando, 1995, p. 865.
[27] Koma, N., Baba, Y., and Matsuoka, K., 1995, *Dig. Tech. Pap.*, SID International Symposium, Orlando, 1995, p. 869.
[28] Vithana, H., Fung, Y. K., Jamal, S. H., Herke, R., Bos, P. J., and Johnson, D. L., 1995, *Dig. Tech. Pap.*, SID International Symposium, Orlando, 1995, p. 873.
[29] Hashimoto, T., Sugiyama, T., Katoh, K., Saito, T., Suzuki, H., Iimura, Y., and Kobayashi, S., 1995, *Dig. Tech. Pap.*, SID International Symposium, Orlando, 1995, p. 877.
[30] Lien, A., John, R. A., Angelopoulos, M., Lee, K. W., Takano, H., Tajima, K., Takenaka, A., Nagayama, K., Momoi, Y., and Saitoh, Y., 1995, Proceedings of the 15th International Display Research Conference (SID, Hamamatsu, 1995), p. 593.
[31] Sugiyama, T., Hashimoto, T., Katoh, K., and Kobayashi, S., 1995, *Jpn. J. appl. Phys.*, **34,** 2396.
[32] Murai, H., Suzuki, M., and Kaneko, S., 1996, Proceedings of the 16th International Display Research Conference (SID, Birmingham, 1996), p. 159.
[33] Bos, P. L., and Rahman, J. A., 1993, *Dig. Tech. Pap.*, SID International Symposium, Seattle, 1993, p. 273.
[34] Yamaguchi, Y., Miyashita, T., and Uchida, T., 1993, *Dig. Tech. Pap.*, SID International Symposium, Seattle, 1993, p. 277.
[35] Miyashita, T., Yamaguchi, Y., and Uchida, T., 1995, *Jpn. J. appl. Phys.*, **34,** 177.
[36] Kiefer, R., Weber, B., Windsceid, F., and Baur, G., 1992, Proceedings of 12th International Display Research Conference (SID, Horoshima, 1992), p. 547.
[37] Oh-e, M., and Kondo, K., 1995, *Appl. Phys. Lett.*, **67,** 3895.
[38] Oh-e, M., and Kondo, K., 1997, *Liq. Cryst.*, **22,** 379.
[39] Oh-e, M., and Kondo, K., 1996, *Appl. Phys. Lett.*, **69,** 623.
[40] Oh-e, M., Yoneya, M., Ohta, M., and Kondo, K., 1997, *Liq. Cryst.*, **22,** 391.
[41] Oh-e, M., Yoneya, M., and Kondo, K., 1997, *J. appl. Phys.*, **82,** 528.
[42] Oh-e, M., and Kondo, K., 1997 *Jpn. J. appl. Phys* **36,** 6798. .
[43] Sasaki, A., and Uchida, T., 1986, Proceedings of the 6th International Display Research Conference (SID, Tokyo, 1986), p. 62.
[44] Matsumoto, S., Hatoh, H., and Murayama, A., 1989, *Liq. Cryst.*, **5,** 1345.
[45] Weber, G., Finkenzeller, U., Gellhaar, T., Plach, H. J., Rieger, B., and Pohl, L., 1989, *Liq. Cryst.*, **5,** 1381.
[46] Bahadur, B., 1990, *Liquid Crystals Applications and Uses*, Vol. 1 (Singapore: World Scientific).
[47] Demus, D., Goto, Y., Sawada, S., Nakagawa, E., Saito, H., and Tarao, R., 1995, *Mol. Cryst. liq. Cryst.*, **260,** 1.
[48] Schadt, M., Buchecker, R., and Villiger, A., 1990, *Liq. Cryst.*, **7,** 519.
[49] Goto, Y., Ogawa, T., Sawada, S., and Sugimori, S., 1991, *Mol. Cryst. liq. Cryst.*, **209,** 1.
[50] Plach, H. J., Weber, G., and Rieger, B., 1990, *Dig. Tech. Pap.*, SID International Symposium, Las Vegas, 1990, p. 91.
[51] Plach, H. J., Bartmann, E., Poetsch, E., Naemura, S., and Rieger, B., 1992, *Dig. Tech. Pap.*, SID International Symposium, Boston, 1992, p. 13.
[52] Tarao, R., Saito, H., Sawada, S., and Goto, Y., 1994, *Dig. Tech. Pap.*, SID International Symposium, San Jose, 1994, p. 233.
[53] Oh—e, M., Ohta, M., Kondo, K., and Oh-hara, S., 1994, Abstracts of 15th International Liquid Crystal Conference, Budapest, 1994, No. K-P17.
[54] Lee, S. H., You, J. G., Kim, H. Y., Lee, D. S., Kwon, S. K., Park, H. S., and Kim, C. K., 1997, *Dig. Tech. Pap.*, SID International Symposium, Boston, 1997, p. 711.
[55] Ohta, M., Yoneya, M., and Kondo, K., 1996, Proceedings of the 16th International Display Research Conference (SID, Birmingham, 1996), p. 49.
[56] Yoneya, M., Ohta, M., Oh-e, M., and Kondo, K., 1997, *Proc. SPIE.*, **3014,** 40.
[57] Leslie, F. M., 1970, *Mol. Cryst. liq. Cryst.*, **12,** 57.
[58] Chandrasekhar, S., 1977, *Liquid Crystals* (Cambridge: Cambridge University Press).